Spring 2018

Distributed fiber optic sensors for monitoring spatially continuous strain and quasi-distributed refractive index using optical frequency domain reflectometry

Sasi Jothibasu

DISTRIBUTED FIBER OPTIC SENSORS FOR MONITORING SPATIALLY

CONTINUOUS STRAIN AND QUASI-DISTRIBUTED REFRACTIVE INDEX

USING OPTICAL FREQUENCY DOMAIN REFLECTOMETRY

by

SASI JOTHIBASU

A THESIS

Presented to the Faculty of the Graduate School of the

MISSOURI UNIVERSITY OF SCIENCE AND TECHNOLOGY

In Partial Fulfillment of the Requirements for the Degree

MASTER OF SCIENCE IN ELECTRICAL ENGINEERING

2018

Approved by

Dr. Jie Huang, Advisor
Dr. Steve Watkins
Dr. Ian Ferguson

PUBLICATION THESIS OPTION

This thesis has been prepared in the form of two papers:

Paper I, pages 2-18 are intended for submission to IOPSCIENCE Measurement Science and Technology.

Paper II, pages 19-34 has been published in Sensors and Actuators B: Chemical, April 2017.

ABSTRACT

This thesis is comprised of two papers and they describe distributed fiber optic sensing using an optical frequency domain reflectometry (OFDR) instrumentation system.

The first paper presents about distributed fiber optic sensor embedded within the layers of a composite laminates to monitor the continuous profile of strain using the optical frequency domain reflectometry (OFDR) system. The OFDR system was used to analyze the Rayleigh backscattered signal. The shift in the Rayleigh backscattered spectrum (RBS) was observed to be linearly related to the change in strain of the composite material. The continuous strain sensing using OFDR was demonstrated by an INSTRON tensile testing system and cantilever beam experiment. The results shows a good strain transfer between the composite laminate and the optical fiber with no slipping or hysteresis issues.

The second paper of the thesis proposes and demonstrates the distributed refractive index sensing by a macrobending single mode fiber (SMF) and the OFDR system. The macro-bending fiber is fabricated by bending a piece of SMF to a particular radius of curvature in several millimeters. The refractive index (RI) of the external medium surrounding the macrobending fiber is measured by the RBS shift using OFDR system. RI is measured from the range of 1.3348 to 1.3557 using the proposed method in our experiment. This sensor can also be used to detect multipoint RIs simultaneously verifying the capability of distributed sensing.

ACKNOWLEDGMENTS

Firstly, I would like to express my sincere gratitude to my advisor, Dr. Jie Huang, for his patience, guidance, encouragement, and support throughout the study of my masters'. His dispassionate commitment to research and hard work are the two motivating factors that kept me going through out my masters' and gain immense knowledge both practically and theoretically. I would also like to thank my committee members Dr. Steve Watkins and Dr. Ian Ferguson for their guidance and support.

Secondly, I would like to thank University of Missouri Research Board and Materials Research Center at Missouri S&T funding societies for providing funds.

Also, I would like to acknowledge my post-doc Yang Du and my lab mates for the valuable discussions and their inputs.

Last but not least I would like to express my very profound gratitude to my parents, sister and friends for believing in me and for their unfailing support and continuous encouragement.

TABLE OF CONTENTS

Page

SECTION

LIST OF ILLUSTRATIONS

SECTION

1. INTRODUCTION

Fiber optic sensors (FOSs) used for real-time structural health monitoring (SHM) have gained considerable interest due to the advantages such as compact size, lightweight, easy embedment, wide operating temperature range, multiplexing capabilities, and immunity to electromagnetic interference. FOSs can be used either as localized sensors or as distributed sensors, and they are used to sense strain, temperature, refractive index, etc. Optical frequency domain reflectometry (OFDR) is a distributed fiber optic sensing technique which can achieve very high sensitivity and high spatial resolution. Here, we have demonstrated an OFDR system for aquiring Rayleigh backscattering signals from an optical fiber for distributed sensing applications

First part of the thesis deals with the OFDR system monitoring the continuous profile of strain in composite laminates, by embedding a distributed sensor within the layers of the composite material. The optic fiber used is a standard single mode fiber. The OFDR system is set to configure a spatial resolution of 1 cm, and can measure a minimum strain of 1 $\mu\varepsilon$. The integration of distributed sensors in composite materials is demonstrated by using an INSTRON tensile testing system and cantilever beam experiment.

Second part of the thesis talks about the OFDR system that monitors the refractive index (RI) by a macrobending single mode fiber. We can use this sensor to detect the multi-point RI to verify the capability of distributed sensing. Also the fiber has the buffer coating remaining which makes the fiber robust in practical applications such as environmental, biological, or chemical measurement and maintain its mechanical property.

PAPER

I. SPATIALLY CONTINOUS STRAIN MONITORING OF CARBON FIBER COMPOSITES USING EMBEDDED DISTRIBUTED FIBER OPTIC SENSORS

Sasi Jothibasu[1], Yang Du[1], Sudharshan Anandan[2], Gurjot S. Dhaliwal[2], Rex E. Gerald II[3], K. Chandrashekhara[2] and Jie Huang[1*]

[1]Department of Electrical and Computer Engineering, Missouri University of Science and Technology, Rolla, MO 65401, USA
[2]Department of Mechanical and Aerospace Engineering, Missouri University of Science & Technology, Rolla, MO 65409, USA.
[3]American Inventor Institute, Willow Spring, IL 60480, USA

*Email: jieh@mst.edu

ABSTRACT

A distributed fiber optic strain sensor based on Rayleigh backscattering, embedded in a fiber reinforced polymer composite, has been demonstrated. The optical frequency domain reflectometry (OFDR) technique was used to analyze the backscattered signal. The shift in the Rayleigh backscattered spectrum (RBS) was observed to be linearly related to the change in strain of the composite material. The sensor (standard single mode fiber) was embedded in between the layers of the composite laminate. A series of tensile loads were applied to the laminate using an Instron testing machine, and the corresponding strain distribution of the laminate was measured. The results show a linear response indicating a seamless integration of the optic fiber in the composite material and a good correlation with the strain gauge results. The sensor was also used to evaluate the strain response of a composite laminate based cantilever beam. In this study, distributed strain measurements in a composite laminate were successfully obtained using an embedded fiber optic sensor.

1. INTRODUCTION

Composite materials are extensively used in various fields such as the aerospace, the automotive, wind turbines, shipping, sports, and the recreation market. These advanced materials have advantages, such as low density, high specific strength and stiffness, good vibration damping, long fatigue life, high wear, corrosion resistance, temperature resistance, and strong tailorability [1-4]. Structural composites in these applications can be subjected to heavy loads and extreme service conditions. Non-destructive techniques such as ultrasonic testing, radiography, thermography, eddy current testing, etc. can be used to detect damage in a composite laminate. However, these techniques are difficult to use due to the need for heavy equipment and intensive labor [1]. Structural health monitoring (SHM) can be used to prevent the onset of damage and catastrophic failure. Sensors such as strain gauges, piezoelectric sensors [5], MEMs sensors and fiber optic sensors [6] are commonly used for SHM of composite materials [7]. A disadvantage of using the strain gauges and piezoelectric sensors is that they are susceptible to electromagnetic interference (EMI) [7]. Also, most of the sensors above are capable of sensing only localized strains or operate at a limited temperature range.

Fiber optic sensors (FOSs), when compared to other sensors, exhibit many advantages like immunity to EMI, wide operating temperature range, compact size, low cost, light weight, and easy embedment. [7]. FOSs are used to sense temperature, strain, and refractive index, either as localized sensors or as distributed sensors. Standard fiber Bragg gratings (FBGs)[8,9], interferometric fiber optic sensors [10], fiber optic micro bend sensors, distributed sensors, and hybrid sensors [11] are some of the different types of fiber optic sensors [7]. Multiplexed sensing is achieved by combining and arranging many

discrete sensors along the length of the optic fiber for multiple point strain and temperature sensing. Hybrid sensors simultaneously measure strain, temperature, and thermal strain of the composite materials by combining and arranging different sensors in a single fiber [11]. FBGs can be multiplexed, and a multiplexed FBG is known as multi-point sensor or quasi-distributed sensor [7]. However, strain build up at potential blind spots (e.g., in between two consecutive FBGs) cannot be measured using these point sensors as they are not continuous. Distributed sensors are used for continuous profile monitoring with the fiber itself as a sensor based on Brillion scattering, Raman scattering (inelastic), and Rayleigh scattering (elastic) [7,12]. The advantage of distributed sensing over multiplexed point sensing is that spatially continuous measurement without dark zones can be achieved [13]. Also, since no external modifications are made to the fiber, long distance sensing of temperature and strain can be measured [13]. Rayleigh backscattering (elastic) is due to random refractive index changes along the length of the optic fiber. Rayleigh scattering along an optical fiber can be modeled as a series of Bragg grating sensors located along the length of the fiber [2]. Based on Rayleigh scattering, distributed fiber optic sensing is categorized as optical time domain reflectometry (OTDR) and optical frequency domain reflectometry (OFDR) [14, 17-19]. OFDR can achieve very high sensitivity and high spatial resolution unlike OTDR which cannot achieve high spatial resolution which is the main disadvantage.

There has been significant interest in embedding fiber optic sensors in composite laminates in recent years. Many recent studies demonstrate the popularity of SHM of composites using FOS by surface bonding of the optic fiber. For example, multiplexed FBGs and distributed fiber optic sensing using OFDR were used to monitor dynamic strain

and fatigue damage monitoring of a composite axial fan blade and composite step lap joint respectively by attaching the fiber on the top and bottom surfaces [20, 21]. Hand-layup and pre-preg layup are some of the methods to embed the fiber optic sensor in the intermediate layers of the composite laminate [22]. There are many techniques like braided composites embedded with FOS, and FOS stitched carbon fiber preforms for advanced composite structures that employ the embedding of FOS inside the composite structure to maintain structural integrity [23, 24]. Examples are reported describing the successful embedment of polarimetric sensors [25], fiber Bragg grating sensors [8], photonic crystal fiber interferometric sensors [10], and hybrid sensors [11] in composite laminates. The FOS reported in these examples are point sensors that are embedded in the intermediate layers of composite. In the traditional surface bonded OFDR based distributed strain sensing technique, it cannot accurately reveal the internal strain profile of the composite laminates which are critical in composite material design. OFDR-based distributed sensing using optic fibers embedded inside composite materials remains to be explored.

In the current work, a spatially continuous distributed fiber optic sensor was embedded within the layers of composite laminates to monitor the continuous profile of strain using the OFDR system. This paper has the uniqueness of OFDR strain sensing using the optic fibers which are embedded inside the composite samples unlike the surface bonding. The carbon fiber/ epoxy composite samples were manufactured by the out-of-autoclave (OOA) technique, using six layers of IM7/Cycom 5320-1 prepreg. The OFDR system can achieve a spatial resolution of 1 cm, and can measure a minimum strain of 10 $\mu\varepsilon$. The optic fiber used is a standard single mode fiber. The OFDR technique was used to analyze the backscattered signal. The shift in the Rayleigh backscattered spectrum (RBS)

is linearly related to a change in strain in the composite materials. This work shows the seamless integration of distributed sensors in composite materials by demonstrating continuous strain sensing using an INSTRON tensile testing system and cantilever beam experiment.

2. METHODOLOGY

2.1 COMPOSITE SAMPLE FABRICATION

The composite samples were manufactured according to the schematic shown in Figure 1(a), by the out-of-autoclave (OOA) technique, using six layers of the IM7G/Cycom5320-1 prepreg system (Figure 1(b)). Prepreg layers were cut to a nominal size of 12 in. x 3 in. (304.9 mm x 76.2 mm) and laid on an aluminum mold. The compacted thickness of the samples was found to be 0.059 in. (1.5 mm). A standard single mode FOS was embedded between the central layers of the composite sample. The placement of FOS was important because if improperly done, it can produce local distortions causing structural performance degradation [8]. Heat shrink-tubes were used at the ingress and egress points to prevent damage to the optic fiber due to high-stress concentrations (Figure 1(a)).

The prepreg layup was cured as per the manufacturer recommended cure cycle at a vacuum pressure of 28 in. Hg. A two-step cure cycle was used to cure the composite (Figure 1(c)). The layup was first heated to 140 °F (60 °C) to maximize the mobility of the reacting groups, and then cured at 265 °F (129.4 °C). The sample was then subjected to a free-standing post cure at 350 °F (177 °C) for 2 hours. The manufacturing procedure was used

to fabricate 6 layer cross-ply and unidirectional composite samples with embedded fiber optic sensors.
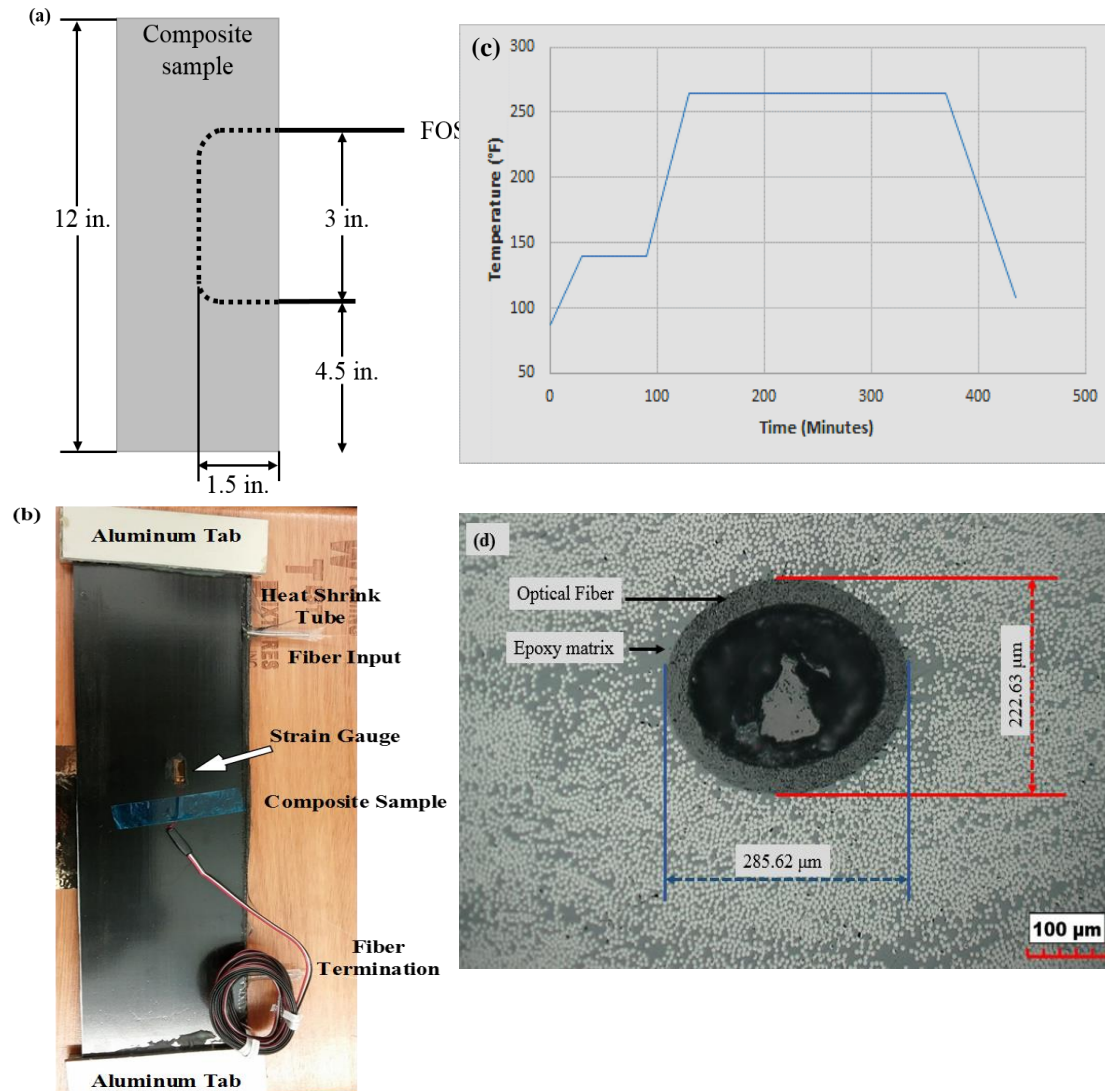
Figure 1. (a) Schematics of an optic fiber embedded in a composite sample (b) Photograph of composite sample with the strain gauge attached on surface (c) Manufacturer recommended cure cycle for IM7G/Cycom5320-1 prepreg system (d) Cross-section image of Optical fiber embedded in the unidirectional composite.

Figure 1(d) shows the cross-section image of an optic fiber being embedded in the unidirectional composite laminate. The clear interface between the optic fiber and the

epoxy matrix is observed in the figure. The diameter of the outer cylinder in Figure 1(d) is the outer coating of an optical fiber (250 µm). It was compressed a little in the horizontal direction (285 µm) making the cross-section of the optic fiber appear like an oval shape instead of a circle. The reason for the compression is the composite laminate manufacturing conditions where the composite material and the embedded sensor is subjected to high temperature and pressure in the horizontal direction (265 °F and 28 In. Hg respectively). However, the compression of the coating layer of the optical fiber does not influence the sensor behavior since the light signal is confined to the fiber core. Also, the continuous interface formed between the epoxy matrix material and the optical fiber could result in a good strain transfer between the composite and optical fiber.

2.2. OFDR THEORY AND MEASUREMENT PRINCIPLE

The distributed sensing approach used in the current work is based on Rayleigh backscattering. An OFDR system can be used to sense a continuous profile of temperature and strain [2, 14-16]. The OFDR system can achieve very high sensitivity and spatial resolution but there is a trade-off between measurement resolution, spatial resolution, and sampling rate for the scattering based distributed sensing techniques. Initially, the reference signal was recorded using a few scans of the OFDR system, and then the measured signal was used to analyze the RBS. The optical frequency domain signal obtained was converted into a spatial domain signal through a Fast Fourier Transform (FFT). A sliding window (Δx) is used for the entire range of frequencies, and each window was converted back to the optical frequency domain. Cross-correlation of the reference signal and the measured

signal was done to check the spectral shift of the backscattered spectrum, which corresponds to the change in strain.

The experimental setup for displaying distributed strain measurement of the embedded fiber in a composite laminate using the OFDR technique is shown in Figure 2.
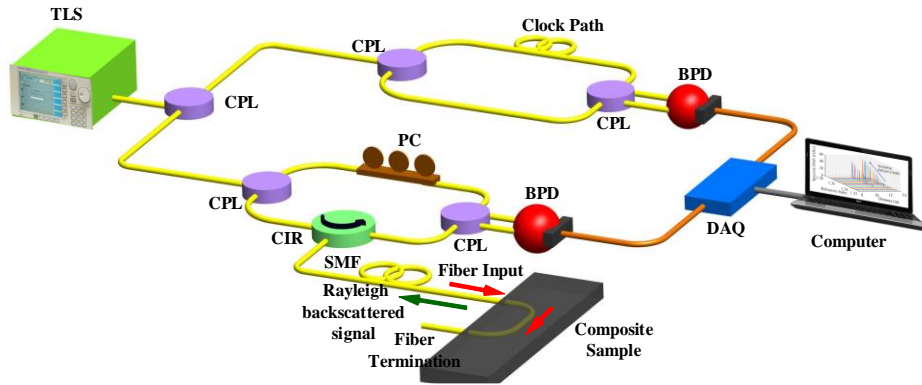
Figure 2. Experimental setup for distributed strain measurement of the embedded fiber in   a composite laminate. TLS: tunable laser source, CPL: coupler, CIR: circulator, PC: polarization controller, BPD: balanced photodetector, DAQ: data acquisition card.

The tunable laser source was used as the light source for the OFDR system. The light from the source was split and takes two paths. One path is through the Auxiliary Interferometer, and the other path is through the Main Interferometer. The Auxiliary Interferometer is a Mach-Zehnder interferometer, which was used to provide an external clock for the Data Acquisition Card (DAQ). It solves the problem of the non-linear effect of the tunable laser, which scans the frequency range and gives the correct time base correspondingly to the DAQ [12, 17]. The light through the main interferometer splits and takes a reference path and a signal path by making use of a coupler. The signal path has the circulator whose one arm has the fiber under test (FUT) which was embedded in the composite laminate. The Polarization Controller was used in the reference arm to modify

the state of light. The backscattered light from the FUT was collected using the same coupler. The reference and the backscattered light was combined using a coupler and detected using the Balanced Photo Detector (BPD).

2.3. EXPERIMENTS

The composite laminate with the embedded FOS was tested for continuous distributed strain sensing under tensile loads. Aluminum tabs (3 in. x 1 in.) were attached to the ends of the composite samples using adhesive structural epoxy adhesive. Three replicates of both unidirectional and cross-ply samples were tested. The testing was done using an Instron 5985 universal testing machine, as shown in Figure 3. The tensile testing was performed using the strain rate of 0.05 in. /min (1.27 mm/min.). Samples were tested up to 600 $\mu\varepsilon$, which is below the failure threshold of the composite. Importantly, the embedded FOS was employed for a range of strain measurements that were well below the known upper limit (8000 microstrains) for reproducible strain measurements by optic fiber sensors [26-29]. The signals were recorded using a DAQ. Signal processing of the Rayleigh-backscattered spectra was done to analyze and study the strain in the composite. A strain gauge was fixed at the center of the composite sample to compare the results with our OFDR system, which gives the continuous strain values along the length of the fiber.
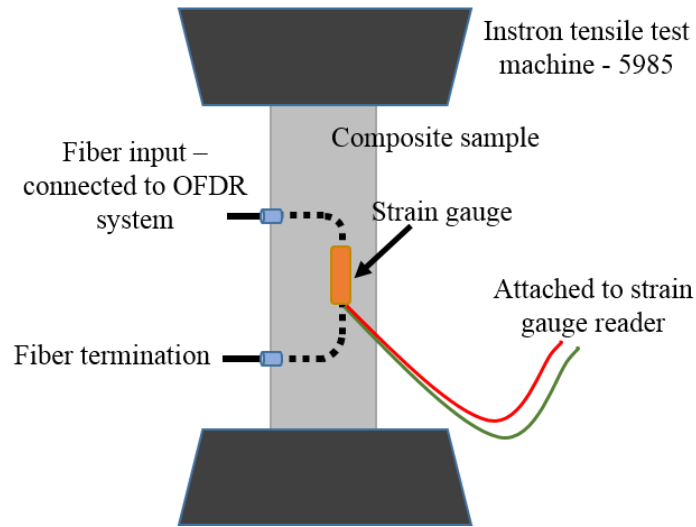
Figure 3. Tensile testing of composite sample using the Instron machine.

After testing the composite sample with Instron test machine, a cantilever beam experiment was conducted to evaluate the distributed strain sensing capability of an optic fiber embedded in a composite sample. Figure 4 shows the composite sample fixed in a cantilever beam-like structure. One end was clamped and the force was applied on the other end of cantilever beam in negative z direction. The optic fiber was embedded under the uppermost layer of the composite specimen to measure strain under cantilever type loading. The end of the cantilever beam was displaced up to 25 mm and the resultant strain was recorded.
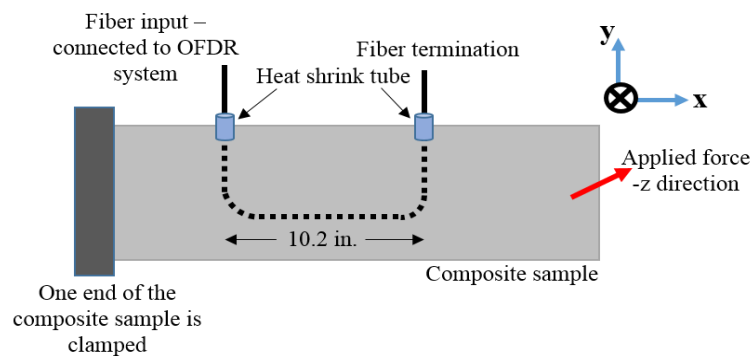
Figure 4. Distributed strain testing of a composite sample using a cantilever experiment.

3. RESULTS AND DISCUSSION

In this section, the results of continuous strain monitoring during of the composite samples under tensile loading are presented. Cross-ply layup composite sample and unidirectional composite sample correspond to sample A and sample B, respectively. Figures 5 (a, b, c, d) show the distributed sensing of the optic fiber embedded along the composite sample with a spatial
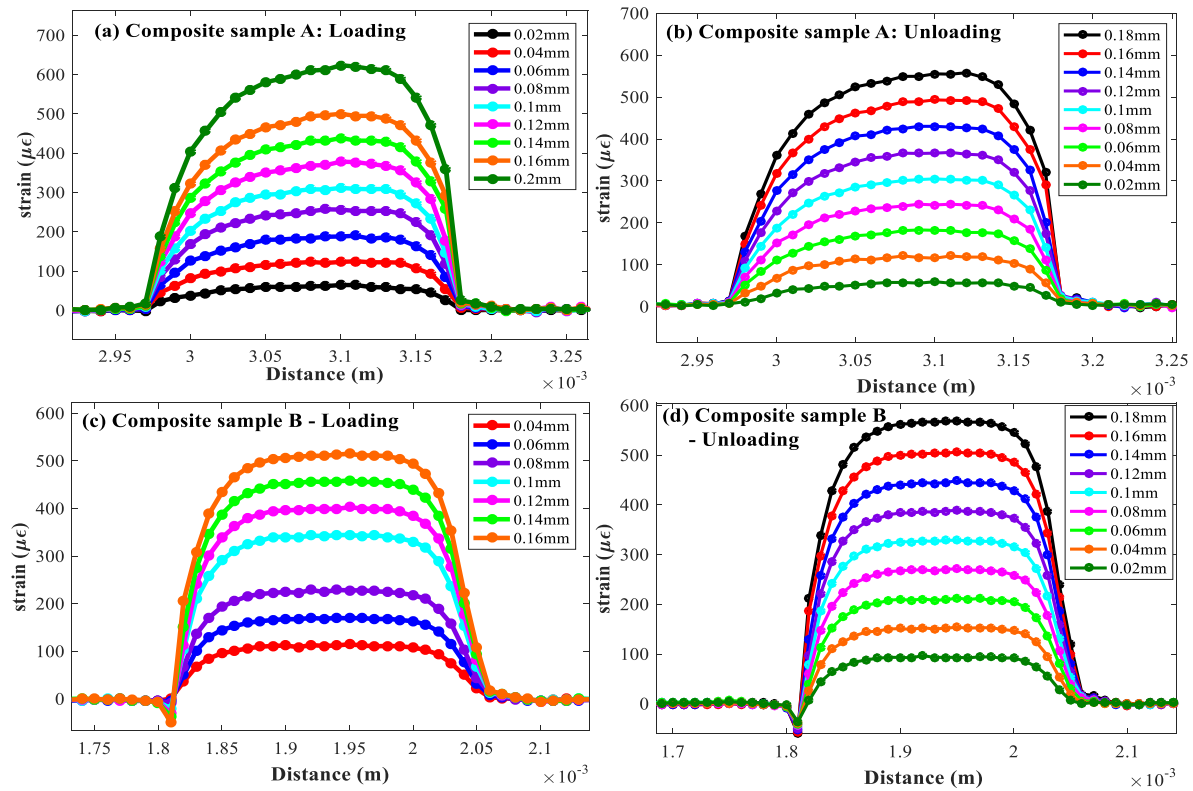
Figure 5. Distributed strain response of the optic fiber embedded in: (a) composite sample A while loading; (b) composite sample A while unloading; (c) composite sample B while loading; (d) composite sample B while unloading.

resolution of 1cm. Loading and unloading was performed in a stepwise manner and strain was monitored using the fiber optic sensor. The loading and unloading curves follow closely to each other, which infer a good embedment of the fiber in the sample. As shown in Figure 5(a), the strain increases as the applied displacement increases. The maximum strain of 600 με is observed when

the applied displacement is 0.2 mm, as shown in Figures 5(a, b, c, d). The distributed strain drops to zero at the beginning and end of the graph because of the shape of the optic fiber embedment in the composite sample as shown in the figure 5. Optic fiber measures strain in the in-plane direction only. The distributed strain values in the composite sample A, is slightly asymmetric or not flat compared to the composite sample B. It may be due to a slight variation in the orientation of the fiber embedded inside the composite laminate, compared to the axis of loading. This can be avoided if careful placement of the fiber using a curve-shaped structure is employed. The fiber in other locations other than the composite seems to be flat which shows the stability of the system with no crosstalk from the composite sensing region. The negative strain, approximately at 1.8 m in composite sample B (Figure 5 (c, d)), can be due to localized stress concentration at the edges of the sample.
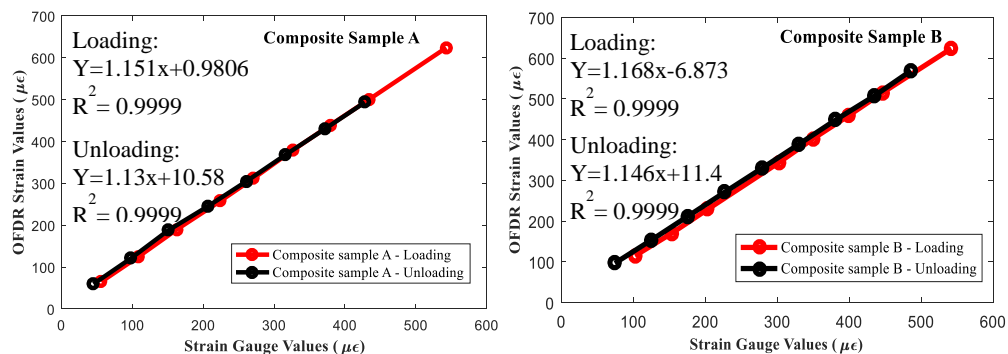
Figure 6. Comparison of strain gauge values and maximum strain OFDR values for loading and unloading (a) for composite sample A, (b) for composite sample B.

The distributed strains measured by the optic fiber are compared to the strain gauge output as shown in figures 6(a, b). A polynomial fitting of degree 1 is applied to the experimental data. From figures 6 (a, b), It is found that the experiment shows a good linearity between the strain gauge values and OFDR strain values for both loading and unloading conditions of the composite samples A and B. The values of R-squared are

mostly 0.999 for all the samples. The slope of the curves while unloading in both the samples is slightly decreased to 2 % when compared to the slope of the loading, but significantly it follows each other. This shows a good strain transfer between the composite laminate and the optical fiber.

The results from the cantilever experiment in figures 7 (a, b) show a good linear response. The initial increase of strain values from 3.9 meters to 4.05 meters is due to the curved embedding of the fiber with heat shrink tubes in the sample. We have the maximum strain of approximately 500 με at 4.06 meters (Figures 7 (a, b)) which is the starting point of the cantilever beam. As expected, the strain readings decrease along the length of the
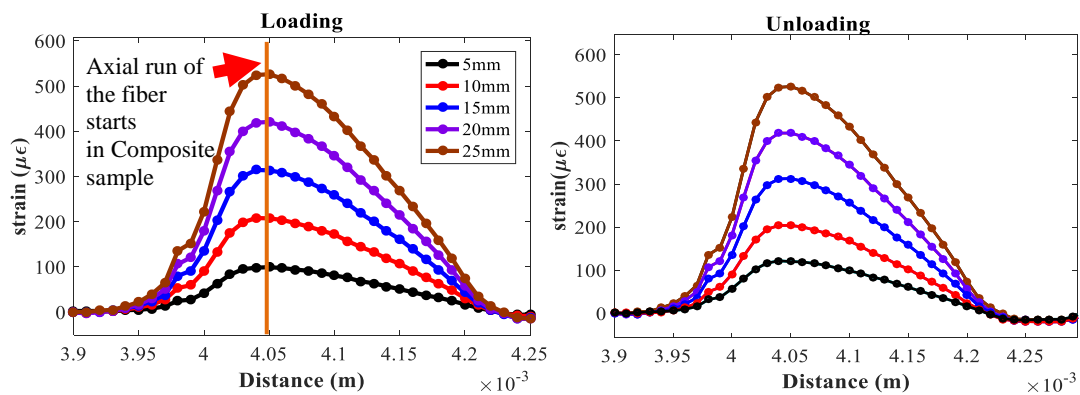
Figure 7. Distributed strain testing of a composite laminate using a cantilever experiment, distributed strain values using OFDR while (a) loading (b) unloading.

beam. The decrease in strain is picked up by the optical fiber. The loading and the unloading values match each other which demonstrate the seamless integration of the optic fiber in the composite sample with no slipping or hysteresis issues. It should be noted that the little compression of the optical fiber shown in microscopic image in Figure 1(d) has not affected the Rayleigh backscattered signal, which is an advantage of the OFDR system.

4. CONCLUSION

Distributed strain sensing in composite materials using OFDR has been demonstrated. Single mode optic fiber embedded within the layers of a composite laminate has been used as a sensor. The shift in Rayleigh backscattered signal is proportional to change in strain in the composite material. This has been validated using tensile testing machine and a cantilever beam experiment. The results show a linear response between the applied displacement and the measured strain. The results were validated using a strain gauge bonded to the surface of the tensile test sample. Periodic structural health monitoring helps identify locations of stress concentration, paths of stress propagation, and areas subjected to fatigue. This data helps to reinforce and repair the affected areas avoiding catastrophic failure well in advance. The proposed technique in this paper monitors the health continuously with a spatial resolution of 1 cm. OFDR based distributed strain sensing with the optic fiber embedded in the intermediate layers of composites is a unique idea and can be very useful for structural health monitoring. This work can be extended to simultaneous measurement of both strain and temperature for the FOS embedded in the composite material in future studies.

REFERENCES

1. Cai J, Qiu L, Yuan S, Shi L, Liu P, Liang D. Structural health monitoring for composite materials. InComposites and Their Applications 2012. InTech.

2. Chen Z, Yuan L, Hefferman G, Wei T. Ultraweak intrinsic Fabry–Perot cavity array for distributed sensing. Optics letters. 2015 Feb 1;40(3):320-3.

3. Anandan S, Nagarajan S, Kaur A, Chandrashekhara K, and Xiao H. Monitoring of out-of-autoclave BMI composites using fiber optic sensors. Proceedings of the SPIE Smart Structures and Materials -Nondestructive Evaluation and Health Monitoring. 2013 May (pp 86940M-86940M)

4. Takeda N. Summary report of the structural health-monitoring project for smart composite structure systems. Advanced Composite Materials. 2001 Jan 1;10(2-3):107-18.

5. Ramos CA, de Oliveira R, Marques AT. Implementation and testing of smart composite laminates with embedded piezoelectric sensors/actuators. InMaterials Science Forum 2008 (Vol. 587, pp. 645-649). Trans Tech Publications.

6. Li HN, Li DS, Song GB. Recent applications of fiber optic sensors to health monitoring in civil engineering. Engineering structures. 2004 Sep 30;26(11):1647-57.

7. Ramakrishnan M, Rajan G, Semenova Y, Farrell G. Overview of fiber optic sensor technologies for strain/temperature sensing applications in composite materials. Sensors. 2016 Jan 15;16(1):99.

8. Murukeshan VM, Chan PY, Ong LS, Seah LK. Cure monitoring of smart composites using fiber Bragg grating based embedded sensors. Sensors and Actuators A: Physical. 2000 Feb 1;79(2):153-61.

9. Lawson NJ, Correia R, James SW, Partridge M, Staines SE, Gautrey JE, Garry KP, Holt JC, Tatam RP. Development and application of optical fibre strain and pressure sensors for in-flight measurements. Measurement Science and Technology. 2016 Sep 16;27(10):104001.

10. Rajan G, Ramakrishnan M, Lesiak P, Semenova Y, Wolinski T, Boczkowska A, Farrell G. Composite materials with embedded photonic crystal fiber interferometric sensors. Sensors and Actuators A: Physical. 2012 Aug 31;182:57-67.

11. Ramakrishnan M, Rajan G, Semenova Y, Farrell G. Hybrid fiber optic sensor system for measuring the strain, temperature, and thermal strain of composite materials. IEEE sensors journal. 2014 Aug;14(8):2571-8.

12. Yuksel K, Wuilpart M, Moeyaert V, Mégret P. Optical frequency domain reflectometry: A review. InTransparent Optical Networks, 2009. ICTON'09. 11th International Conference on 2009 Jun 28 (pp. 1-5). IEEE.

13. Huang J, Lan X, Luo M, Xiao H. Spatially continuous distributed fiber optic sensing using optical carrier based microwave interferometry. Optics express. 2014 Jul 28;22(15):18757-69.

14. Du Y, Liu T, Ding Z, Liu K, Feng B, Jiang J. Distributed magnetic field sensor based on magnetostriction using Rayleigh backscattering spectra shift in optical frequency-domain reflectometry. Applied Physics Express. 2014 Dec 22;8(1):012401.

15. Du Y, Jothibasu S, Zhuang Y, Zhu C, Huang J. Rayleigh backscattering based macrobending single mode fiber for distributed refractive index sensing. Sensors and Actuators B: Chemical. 2017 Sep 30;248:346-50.

16. Du Y, Jothibasu S, Zhuang Y, Zhu C, Huang J. Unclonable Optical Fiber Identification Based on Rayleigh Backscattering Signatures. Journal of Lightwave Technology. 2017 Nov 1;35(21):4634-40.

17. Froggatt M, Moore J. High-spatial-resolution distributed strain measurement in optical fiber with Rayleigh scatter. Applied Optics. 1998 Apr 1;37(10):1735-40.

18. Ukil A, Braendle H, Krippner P. Distributed temperature sensing: review of technology and applications. IEEE Sensors Journal. 2012 May;12(5):885-92.

19. Minardo A, Bernini R, Zeni L, Thevenaz L, Briffod F. A reconstruction technique for long-range stimulated Brillouin scattering distributed fibre-optic sensors: experimental results. Measurement Science and Technology. 2005 Feb 24;16(4):900.

20. Wong L, Chowdhury N, Wang J, Chiu WK, Kodikara J. Fatigue damage monitoring of a composite step lap joint using distributed optical fibre sensors. Materials. 2016 May 14;9(5):374.

21. Di Sante R. Fibre optic sensors for structural health monitoring of aircraft composite structures: Recent advances and applications. Sensors. 2015 Jul 30;15(8):18666-713.

22. Kaur A, Anandan S, Yuan L, Watkins SE, Chandrashekhara K, Xiao H, Phan N. Strain monitoring of bismaleimide composites using embedded microcavity sensor. Optical Engineering. 2016 Mar 1;55(3):037102-.

23. Carman GP, Sendeckyj GP. Review of the mechanics of embedded optical sensors. Journal of Composites, Technology and Research. 1995 Jul 1;17(3):183-93.

24. Lesiak P, Szeląg M, Budaszewski D, Plaga R, Mileńko K, Rajan G, Semenova Y, Farrell G, Boczkowska A, Domański A, Woliński T. Influence of lamination process on optical fiber sensors embedded in composite material. Measurement. 2012 Nov 30;45(9):2275-80.

25. Ramakrishnan M, Rajan G, Semenova Y, Lesiak P, Domanski A, Wolinski T, Boczkowska A, Farrell G. The influence of thermal expansion of a composite material on embedded polarimetric sensors. Smart Materials and Structures. 2011 Nov 4;20(12):125002.

26. Feng A, Chen D, Li C, Gu X. Flat-cladding fiber Bragg grating sensors for large strain amplitude fatigue tests. Sensors. 2010 Aug 16;10(8):7674-80.

27. Hong CY, Yin JH, Pei HF, Huang D. Measurement of cracks in concrete beams using a Brillouin optical time domain analysis sensing technology. In Proceedings of the Second International Postgraduate Conference on Infrastructure and Environment (supplement) Hong Kong 2010 (pp. 22-28).

28. Challener W, Knobloch A, Ajgoankar M, Chamarthy P, Xia H, Jones R, Craddock R, Zhao L, Kinnell P, Sensing GE, Lane FT. Subsystem design and validation for optical sensors for monitoring enhanced geothermal systems. InProceedings of Thirty-Sixth Workshop on Geothermal Reservoir Engineering, Stanford University, Stanford, CA (Vol. 31).

29. Zhou Z, Wang Z, Shao L. Fiber-Reinforced Polymer-Packaged Optical Fiber Bragg Grating Strain Sensors for Infrastructures under Harsh Environment. Journal of Sensors. 2016 Dec 13;2016.

II. RAYLEIGH BACKSCATTERING BASED MACROBENDING SINGLE MODE FIBER FOR DISTRIBUTED REFRACTIVE INDEX SENSING

Yang Du, Sasi Jothibasu, Yiyang Zhuang, Chen Zhu, Jie Huang[*]

Department of Electrical and Computer Engineering, Missouri University of Science and Technology, Rolla, MO 65401, USA

*Email: jieh@mst.edu

ABSTRACT

A novel and compact distributed refractive index (RI) sensor based on Rayleigh backscattering and macrobending single mode fiber (SMF) is proposed and experimentally investigated. Our proposed sensor is simply fabricated by bending a piece of SMF to a radius of curvature in several millimeters. We detect the refractive index of the external medium surrounding the macrobending fiber, for the first time, by analyzing the Rayleigh backscattering signals recorded from optical frequency domain reflectometry. We measure the range of the RI from 1.3348 to 1.3557 using the proposed method. To verify the capability of the distributed sensing, we also use this sensor to detect multipoint RIs simultaneously. The RI measurement sensitivities are 2319.24GHz/RIU (18.55nm/RIU) and 2717.85GHz/RIU (21.74nm/RIU) with bending diameters of 12.2mm and 11.3mm, respectively. In addition, our macrobending fiber has its original buffer coating remaining intact, allowing the fiber to maintain optimal mechanical property and be suitable for more practical applications.

Keywords: Rayleigh backscattering, macrobending, single mode fiber, refractive index, distributed sensing

1. INTRODUCTION

Fiber optics refractive index (RI) sensors have been studied and proposed extensively for biomedical, chemical, industrial and environmental applications over the past decades [1], owing to their well-known advantages such as immunity to electromagnetic interference, compact size, light weight, potential low cost and the possibility of distributed sensing over a long distance [2-6]. Most of the optical fiber based RI sensors work in the principle of interaction of the evanescent field with the external medium. A number of optical fiber RI sensors have been proposed with different structures, such as a long period fiber grating (LPFG) [7] [8], fiber Bragg gratings (FBG) [9], optical fiber surface plasmon resonance (SPR) [10], photonics crystal fiber based sensor [11], Fabry–Perot refractometer [12-14], thin core fiber based sensor [15], in-fiber Mach–Zehnder refractometer [16] or single-mode-multimode-single-mode (SMS) fiber [17-19].

In recent years, an interesting idea of designing an optical fiber based RI sensor is to simply bend a single mode fiber (SMF). This method has attracted considerable interests in RI measurement due to its easy fabrication and high sensitivity. For instance, Sun et al. developed a fiber taper-based modal interferometer with a microfiber bend [20]; a leaky mode interferometer of bend fiber was also presented by Zhang et al. [21]; Chen et al. proposed a RI sensor based on macrobending fiber Bragg grating [22]; Wang et al. introduced a RI sensor based on macrobending single mode fiber by measuring bend loss [23] [24], and they also reported a Whispering Gallery mode based RI sensor, in which high loss fiber was used after removing the buffer coating and bent in the shape of ring [25]. Though some of these techniques can achieve very high RI sensitivity, the sensor fabricated by stripping the coating, polishing, etching, tapering or drilling makes the fiber

more fragile [7-25]. Moreover, most of these methods are point sensors and difficult to realize distributed sensing or multiplexing based on their proposed interrogation methods, showing less interest in practical applications. In addition, the aforementioned RI sensors based on bending structures work in transmission mode, which may limit their practical applications. As such, designing a RI sensor based on bending structure with distributed sensing capability and reflection mode is highly needed.

The macrobending single mode fiber structure is sensitive to changes in refractive index of the external medium. Due to the macrobending of the fiber, the light travelling in the core will be partially coupled into the cladding and therefore generates multiple cladding modes with different orders. An interferogram will be formed due to multimodal interference. It has been approved that this interferogram can be used for ambient RI sensing [26]. Typically, the interferogram is acquired by a broadband source and optical spectrum analyzer, or a scanning laser with a photodetector. It would be difficult to realize distributed sensing based on these conventional interrogation methods. Inspired by the traditional Rayleigh scattering based distributed sensing technology, for the first time, we are considering to use Rayleigh backscattering to acquire the interferogram due to multimodal interference. Potentially, distributed RI sensing with macrobending structures can be achieved based on this method. Rayleigh backscattering is caused by random refractive index fluctuations along an optical fiber, and it can be modeled as a long, weak FBG with random periods [27]. The strain or temperature variation causes a local Rayleigh backscattering spectra (RBS) shift, which can be calculated using the cross-correlation between the measured RBS and a reference RBS [28]. When we combine the technologies of the macrobending single mode fiber and distributed sensing using an RBS shift, a

Rayleigh backscattering based macrobending single mode fiber for distributed refractive index sensing can be developed.

In this paper, we propose and demonstrate a distributed refractive index sensing technology based on Rayleigh backscattering and macrobending single mode fiber. Our proposed sensor can be easily fabricated by bending a piece of SMF to a radius of curvature in several millimeters. We detect the refractive index of the external medium surrounding the macrobending fiber by measuring the RBS shift using optical frequency domain reflectometry (OFDR). In our experiment, we measure the range of the RI from 1.3348 to 1.3557 using the proposed method. We also use this sensor to detect multipoint RIs simultaneously to verify the capability of distributed sensing. In addition, our macrobending fiber has buffer coating remaining which helps to maintain the mechanical property of the sensor and makes it robust in practical applications.

2. STRUCTURE DESIGN AND MEASUREMENT PRINCIPLE

A schematic diagram of Rayleigh backscattering based macrobending single mode fiber is illustrated in Figure 1. The structure of bending fiber is fabricated mechanically with a selected bending diameter. The buffer coating in the bend fiber remains intact to prevent it from braking. Also, it has been proven that the RI variation of the external medium can be detected with the intact coating via our Rayleigh backscattering based method. The two ends of fiber after the bending part are fed through two microtubes with a length of 4cm and inner diameter of 0.5mm, respectively. We use 3M industrial tape to

hold both the microtubes and the fiber on a plastic plate with a length×width of 60×30mm, so the bending structure can be fixed with a certain bending diameter. To verify the
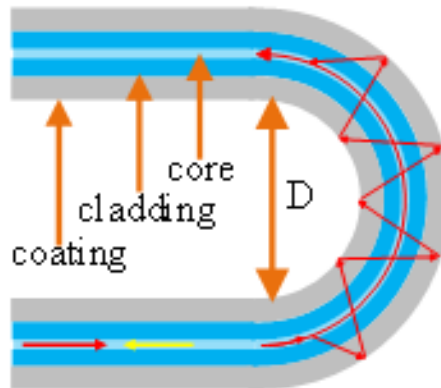

Figure 1. Schematic diagram of bending fiber consisting of core, cladding and coating. D is bending diameter of this structure.

capability of multipoint RI sensing, we make the same structure at another position along this fiber with a different bending diameter. This easy-to-build and robust structure can be easily employed at any position along the whole fiber for distributed RI sensing.

When the light propagates along the straight SMF to the bending section as shown in Figure 1, high order cladding modes confined in the optical fiber itself will be excited, where the light in the core will be coupled to the cladding therefore generates multiple cladding modes with different orders. As we know that the RI of the cladding is lower than the RI of the fiber core. If the RI of the external medium is lower than that of the coating, meanwhile the bending diameter is not too small, the radiated field of total internal reflection will not only occur at the core-cladding boundary but also the coating-surrounding boundary [22] [25] [29]. After the light travels through the bending section, the RI of the external medium modifies the coupling light, the light recoupled to the core mode will interfere with the remaining mode and generate interference fringes in the

spectral domain, an interferogram will be formed due to multimodal interference, which causes a spectral shift in interferogram at this bending section [20] [21] [25] [26]. The Rayleigh backscattering light will also be coupled in the bending section and experience multimodal interference, which could be used for RI measurement. The phase difference between the core and the cladding mode after propagating through the bending section of fiber can be written as $\Delta\Phi = \frac{2\pi}{\lambda}\left(n_{co,eff} - n_{cl,eff}\right)L = (2m+1)\pi$ [21] [22], where $n_{co,eff}$ and $n_{cl,eff}$ are the effective RIs of fundamental core mode and cladding mode, respectively. L is the effective dsflength of bending section, λ is the wavelength. The central wavelength of the dip induced by the macrobending fiber structure can be described as $\lambda_m = \frac{2}{2m+1}\Delta n_{eff} \cdot L$, where $\Delta n_{eff} = n_{co,eff} - n_{cl,eff}$ is the effective RI difference between the core mode and cladding mode, m is an integer. When our bending structure is subjected to external RI perturbation, the Rayleigh backscattering spectra (RBS) shift is $\Delta\lambda = \frac{\delta n_{eff}}{\Delta n_{eff}}\lambda_m$, where δn_{eff} is the variation of Δn_{eff} caused by surrounding RI chage. Thus, RI of external medium can be detected and evaluated by measuring the RBS shift.

The Rayleigh backscattering originates from the random fluctuations in the index profile along the optical fiber and it can be modeled as a long, weak FBG with random periods [27]. The RI variation causes some modification in the local Rayleigh backscattering, which cause a shift in the Rayleigh backscattering spectra (RBS). We can detect the local spectral shift by cross-correlation to realize the RI measurement. The signal processing is similar to that of distributed temperature sensing based on the RBS shift in OFDR [28]. Our signal processing procedure for RI sensing in detail is as following:

a. The reference and measurement signals with different RI values are acquired separately.

b. The signals from the optical frequency domain are converted to the spatial domain by fast Fourier transform.

c. A sliding window with a width of ΔX is used to select the local Rayleigh backscattering.

d. To increase the frequency resolution, the local Rayleigh scattering signal in spatial domain after applying a window function is zero-padded.

e. These selected local Rayleigh backscattering signals are converted back to the optical frequency domain by inverse fast Fourier transform.

f. Cross-correlation is performed between the reference and the measured RBS to obtain the spectral shift. The cross-correlation peak is spectral shift of the local RBS, which reflects the RI variation of external medium.

3. EXPERIMENTS AND DISCUSSIONS

Our experimental setup for the distributed RI measurement is shown in Figure 2. A tunable laser source (TLS, Agilent 81680A) is used as the light source for the interrogation system. The tuning speed, tuning range Δv, and starting wavelength of the TLS are 5×10^3GHz/s (40nm/s), 2.5×10^3GHz (20nm), and 1517nm, respectively. The light from the laser is split into two paths by a coupler. One path leads to the auxiliary interferometer (a Mach-Zehnder interferometer). It provides an external clock to trigger the data acquisition card, which samples the interference signal with equal optical frequency spacing to reduce

the nonlinearity of the frequency tuning of the TLS. The other path is the main interferometer. The fiber under test (FUT) in the main interferometer is composed of a 14m long standard SMF.

In our proposed method, we fabricated two macrobending fiber structures with bending diameter 12.2 mm and 11.3 mm as sensing heads at the locations of 11.2 m and 12.8 m, respectively. Figure 3 is the spatial domain signal of the two bending structures
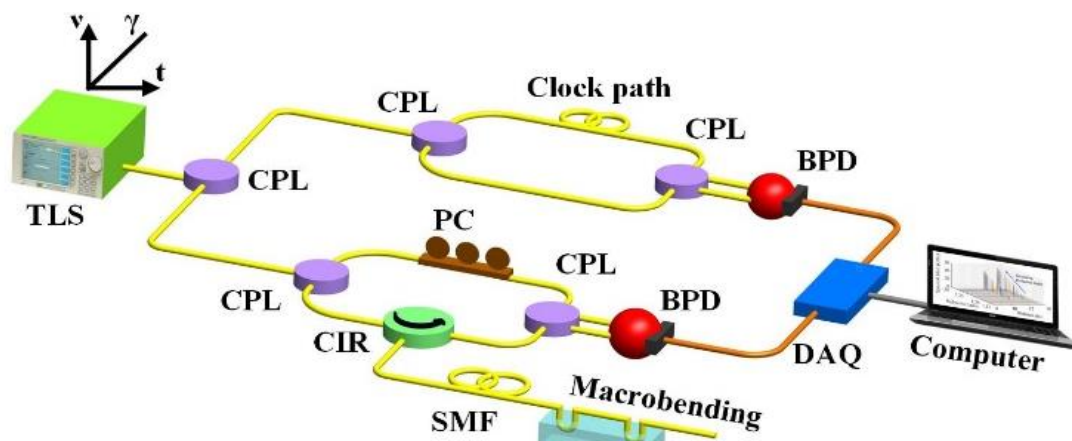

Figure 2. Experimental setup for distributed RI measurement. TLS: tunable laser source, CPL: coupler, CIR: circulator, PC: polarization controller, BPD: balanced photo detector, DAQ: data acquisition card.

After Fourier transform to the recorded OFDR signal. From Figure 3 it can be noted that the bending loss is 4dB generated at the position of 11.2m with bending diameter of 12.2mm, 6dB loss at the position of 12.8m with bending diameter of 11.3mm, respectively. The bending loss is mainly due to the leak of the light at the bending point and the recoupling from cladding modes to core modes. It is obvious that the smaller the bending radius, the higher the bending loss is, as indicated in Figure 3.

To characterize the RI response of our sensor, we immersed the bending structures in ethanol solutions with different RIs. The RIs were modified by changing the concentration of ethanol solution in a clean room with constant temperature of 25°C [30].
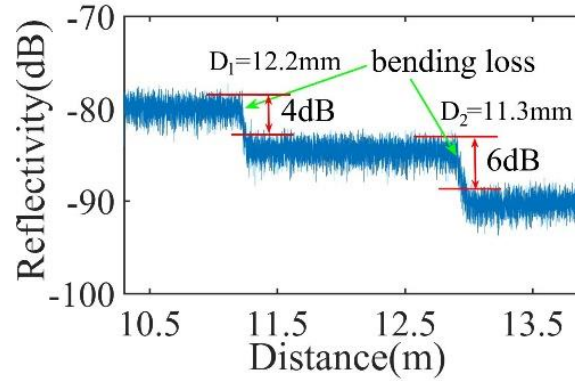

Figure 3. Measured Rayleigh backscattering for a FUT length of 14m. Two bending structures with bending loss 4dB and 6dB at the locations of 11.2m and 12.8m, respectively. Bending diameters of fiber at these two positions are 12.2mm and 11.3mm.

The RI measurement results obtained by the cross-correlation of the RBS are shown in Figure 4. In our experiment, the sliding window with a width of ΔX is the selected length of local Rayleigh backscattering, which can be expressed as $\Delta X = N \cdot \Delta Z$, where N is the number of data points for a local Rayleigh backscattering segment, ΔZ is spatial resolution of the OFDR system and express as $\Delta Z = c/2n_f \Delta v$, c is speed of light in vacuum, n_f is the refractive index of fiber. In this experiment, we use 4cm for ΔX ($N = 1000$, $\Delta Z = 0.004$cm), which could cover the entire length of the two bending fiber structures and can also provide enough measurement sensitivity. When an RI variation $\Delta n = 0.0013$ (RI varies from 1.3354 to 1.3367) at the location of 11.2m was applied, a local Rayleigh backscattering spectral shift of 2.5GHz can be found, as shown in Figure 4(a). When an RI variation $\Delta n = 0.0015$ (RI varies from 1.3410 to 1.3425) at the location of 12.8m was applied, the local Rayleigh backscattering spectral shift of 5GHz can be found, as shown in Figure 4(b). From Figure

4(a) and (b), the macrobending fiber structure with a smaller bending diameter of 11.3mm

is more sensitive than the one with bending diameter of 12.2mm. It is worth mentioning
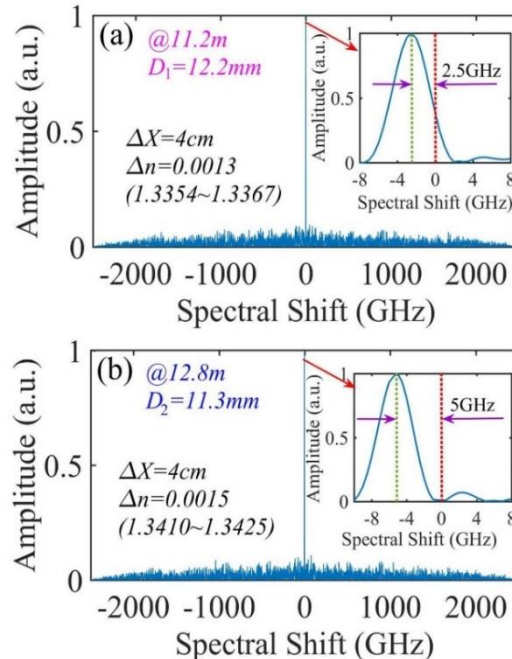

Figure 4. RI measurement based on RBS shift. (a) Cross-correlation of measurement and reference RBS with Δn=0.0013 (RI between 1.3354 and 1.3367) at the position of 11.2m with bending diameter 12.2mm. (b) Cross-correlation of measurement and reference RBS with Δn=0.0015 (RI between 1.3410 and 1.3425) at the position of 12.8m with bending diameter 11.3mm.

that, in our signal processing method, to increase the frequency resolution of the inverse

fast Fourier transform before cross-correlation, the local Rayleigh scattering signal in

spatial domain after applying a window function was zero-padded, which made it easier to

resolve the cross-correlation peak and drastically improved the RI measurement accuracy.

To verify the capability of distributed RI sensing, two bending structures were fabricated

along the fiber at the starting positions of 11.2m and 12.8m with bending diameters of

12.2mm and 11.3mm, respectively. These two bending structures were immersed in a tank
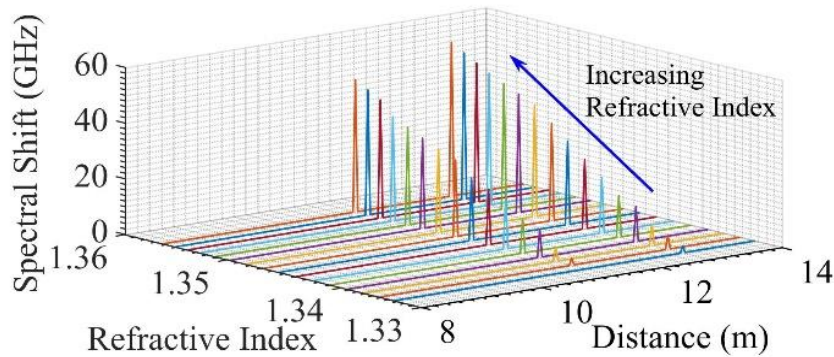
Figure 5. RI measurement using two macrobending structures along the fiber at the starting positions of 11.2m and 12.8m, bending diameters of fiber at these two positions are 12.2mm and 11.3mm, respectively.
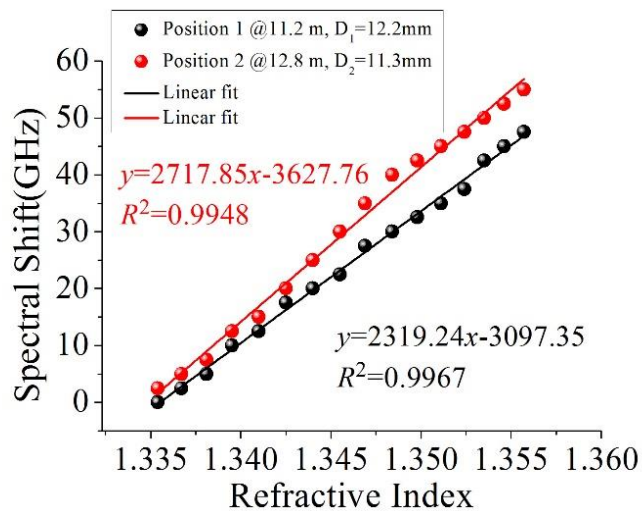
Figure 6. RBS spectral shift at location of 11.2m and 12.8m as a function of RI.

simultaneously in ethanol solutions with different RIs ranging from 1.3348 to 1.3557 as schematically shown in Figure 2. Figure 5 shows the measured spectral shift as a function of distance at various RIs. From the trace, the RBS spectral shifts are detected at the two bending positions with RI variation, and we can find that the RBS spectral shift only occur at the position with bending structures, indicating that there is no any cross-talk from other

fiber sections without bending structures. It can also be found that the RBS spectral shifts increase monotonically with the RI increasing.

RBS spectral shift at location of 11.2m (in black dots) and 12.8m (in red dots) as a function of RI is shown in Figure 6, respectively. A linear fitting is applied to the experimental data. There is a good linear relationship between the RBS shift and the RI for both macrobending structures. The values of R-squared for these two positions can be up to 0.9948 and 0.9967, respectively. This linear fit seems not perfect is due to the environmental temperature fluctuations. Because the refractive index of ethanol solution can be influenced by fluctuations in temperature [31]. The RI sensitivity of the bending fibers with diameter of 12.2mm and 11.3mm are 2319.24GHz/RIU (18.55nm/RIU) and 2717.85GHz/RIU (21.74nm/RIU), respectively. The sensitivity is lower than the ones reported in ref [7-25]. This is because of the remaining of the intact fiber coatings on the bending structures. The macrobending fiber structure at location of 12.8m with a smaller bending diameter has slightly higher sensitivity than the bending structure at 11.2m. Due to different high order modes are excited with different bending diameters and cladding modes propagate with different transmission loss, the sensors are showing different RI sensitivities with different bending diameter. If higher sensitivity is needed in different applications, we can bend the fiber with an acceptable diameter and strip off the polymer coating of the bending section to enhance the interaction between light and the surrounding medium.

4. CONCLUSION

In this letter, we propose a distributed refractive index (RI) sensor based on Rayleigh backscattering and macrobending SMF structures. Our macrobending fiber has its original buffer coating remaining intact, allowing the fiber to maintain optimal mechanical property and be suitable in practical applications. Each macrobending structure has a radius of curvature in several millimeters. RI range from 1.3348 to 1.3557 is detected by measuring the Rayleigh backscattering shift using OFDR. To verify the capability of the distributed sensing, we also detect RIs at multiple locations. The RI sensitivities are 2319.24GHz/RIU (18.55nm/RIU) and 2717.85GHz/RIU (21.74nm/RIU) with bending diameter of 12.2mm and 11.3mm, respectively. To the best of our knowledge, this is the first time that we use Rayleigh backscattering signals to acquire information from multimodal interference for distributed RI measurement. The proposed sensor can be used in several practical applications such as environmental, biological, or chemical measurement, after it is properly calibrated.

REFERENCES

1. O. Wolfbeis, Fiber-optic chemical sensors and biosensors, Anal. Chem. 76 (2004) 3269-3284.

2. I. M. White, X. Fan, On the performance quantification of resonant refractive index sensors, Opt. Express 16 (2008) 1020-1028.

3. Z. Chen, L. Yuan, G. Hefferman, T. Wei, Ultraweak intrinsic Fabry–Perot cavity array for distributed sensing, Opt. Lett. 40(2015) 320-323.

4. Y. Bao, F. Tang, Y. Chen, W. Meng, Y. Huang, G. Chen, Concrete pavement monitoring with PPP-BOTDA distributed strain and crack sensors, Smart Struct. Syst. 18(2016) 405-423.

5. Z. Zhang, Y. Huang, L. Palek, R. Strommen, Glass fiber–reinforced polymer–packaged fiber Bragg grating sensors for ultra-thin unbonded concrete overlay monitoring, Struct. Health. Monit. 14(2015) 110-123.

6. Z. Chen, L. Yuan, G. Hefferman, T. Wei, Ultraweak intrinsic Fabry–Perot cavity array for distributed sensing. Opt. Lett. 40(2015) 320-323.

7. Q. Han, X. Lan, J. Huang, A. Kaur, T. Wei, Z. Gao, H. Xiao, Long-period grating inscribed on concatenated double-clad and single-clad fiber for simultaneous measurement of temperature and refractive index, IEEE Photonics Technol. Lett. 24 (2012) 1130-1132.

8. L. Qi, C. L. Zhao, J. Yuan, M. Ye, J. Wang, Z. Zhang, S. Jin, Highly reflective long period fiber grating sensor and its application in refractive index sensing, Sens. Actuators B Chem, 193 (2014) 185-189.

9. W. Liang, Y. Huang, Y. Xu, R. K. Lee, A. Yariv, Highly sensitive fiber Bragg grating refractive index sensors, Appl. Phy. Lett. 86 (2005) 151122-1-3.

10. D. Monzón-Hernández, J. Villatoro, High-resolution refractive index sensing by means of a multiple-peak surface plasmon resonance optical fiber sensor, Sens. Actuators B Chem. 115 (2006) 227-231.

11. D. K. Wu, B. T. Kuhlmey, B. J. Eggleton, Ultrasensitive photonic crystal fiber refractive index sensor, Opt. Lett. 34 (2009) 322-324.

12. T. Wei, Y. Han, Y. Li, H. L. Tsai, H. Xiao, Temperature-insensitive miniaturized fiber inline Fabry-Perot interferometer for highly sensitive refractive index measurement, Opt. Express, 16 (2008), 5764-5769.

13. O. Frazão, P. Caldas, J. L. Santos, P. V. S. Marques, C. Turck, D. J. Lougnot and O. Soppera, Opt. Lett. Fabry-Perot refractometer based on an end-of-fiber polymer tip, 34 (2009) 2474-2476.

14. J. Zhang, Q. Sun, R. Liang, J. Wo, D. Liu, P. Shum, Microfiber Fabry–Perot interferometer fabricated by taper-drawing technique and its application as a radio frequency interrogated refractive index sensor, Opt. Lett. 37 (2012) 2925-2927.

15. Z. Chen, G. Hefferman, T. Wei, Multiplexed oil level meter using a thin core fiber cladding mode exciter, IEEE Photonics Technol. Lett. 27 (2015): 2215-2218.

16. J. Harris, P. Lu, H. Larocque, L. Chen, X. Bao, In-fiber Mach–Zehnder interferometric refractive index sensors with guided and leaky modes, Sens. Actuators B Chem. 206 (2015) 246-251.

17. Q. Wu, Y. Semenova, P. Wang, G. Farrell, High sensitivity SMS fiber structure based refractometer–analysis and experiment, Opt. Express 19 (2011) 7937-7944.

18. Y. Chen, Q. Han, T. Liu, X. Lü, Self-temperature-compensative refractometer based on singlemode–multimode–singlemode fiber structure, Sens. Actuators B Chem. 212 (2015) 107-111.

19. J. Tang, J. Zhou, J. Guan, S. Long, J. Yu, H. Guan, H. Lu, Y. Luo, J. Zhang, Z. Chen, Fabrication of Side-Polished Single Mode-Multimode-Single Mode Fiber and Its Characteristics of Refractive Index Sensing, IEEE J. Select. Topics in Quantum Electron. 23 (2016) 1-8.

20. L. P. Sun, J. Li, Y. Tan, S. Gao, L. Jin, B. O. Guan, Bending effect on modal interference in a fiber taper and sensitivity enhancement for refractive index measurement,Opt. Express, 21 (2013) 26714-26720.

21. X. Zhang, W. Peng, Fiber optic refractometer based on leaky-mode interference of bent fiber, IEEE Photon. Technol. Lett. 27 (2015) 11-14.

22. Y. Chen, Q. Han, T. Liu, F. Liu, Y. Yao, Simultaneous measurement of refractive index and temperature using a cascaded FBG/droplet-like fiber structure, IEEE Sens. J. (2015) 15, 6432-6436.

23. P. Wang, Y. Semenova, Q. Wu, G. Farrell, Y. Ti, J. Zheng, Macrobending single-mode fiber-based refractometer, Appl. Opt. 48 (2009) 6044-6049.

24. P. Wang, Y. Semenova, Q. Wu, J. Zheng, G. Farrell, Temperature performance of a macrobending single-mode fiber-based refractometer, Appl. Opt. 49 (2010) 1744-1749.

25. P. Wang, Y. Semenova, Y. Li, Q. Wu, G. Farrell, A macrobending singlemode fiber refractive index sensor for low refractive index liquids, Photon. Lett. Poland 2 (2010) 67-69.

26. S. Silva, O. Frazão, J. L. Santos, F. X. Malcata, A reflective optical fiber refractometer based on multimode interference, Sens. Actuators B Chem. 161 (2012) 88-92.

27. M. Froggatt, J. Moore, High-spatial-resolution distributed strainmeasurement in optical fiber with Rayleigh scatter, Appl. Opt. 37(1998), 1735.

28. Y. Du, T. Liu, Z. Ding, Q. Han, K. Liu, J. Jiang, Q. Chen, B. Feng, Cryogenic Temperature Measurement Using Rayleigh Backscattering Spectra Shift by OFDR, IEEE Photon. Technol. Lett. 26 (2014) 1150-1153.

29. A. Harris, P. Castle, Bend loss measurements on high numerical aperture single-mode fibers as a function of wavelength and bend radius, J. Lightwave technol. 4(1986) 34-40.

30. R. L. David, CRC Handbook of Chemistry and Physics, Inter-net Version 2015, 95th ed., Taylor and Francis, Boca Raton, FL, 2015, pp. 8-63. Available: http://www.hbcpnetbase.com

31. G. L. Klunder, J. Bürck, H. J. Ache, R. J. Silva, R. E. Russo,. Temperature effects on a fiber-optic evanescent wave absorption sensor. Appl. Spectrosc. 48(1994) pp.387-393.

ACKNOWLEDGMENTS

SECTION

2. CONCLUSION

Distributed strain sensing in composite materials and sensing of refractive index using OFDR system has been experimentally demonstrated. Strain sensing in composite materials could play an important role in structural health monitoring of the composite structures that are extensively used in various fields such as the aerospace, the automotive, wind turbines, shipping, sports, and the recreation market. SHM helps to identify locations of stress concentration, paths of stress propagation, and areas subjected to fatigue. This data helps to reinforce and repair the affected areas avoiding catastrophic failure well in advance. This work can be extended to simultaneous measurement of both strain and temperature for the FOS embedded in the composite material in future studies. The refractive index sensor can be used in several practical applications such as environmental, biological, or chemical measurement, after proper calibration of the sensor.

VITA

Sasi Jothibasu was born in Tamil Nadu, India. She received her Bachelor of Engineering degree in Electronics and Communication Engineering in June 2015 from Anna University, Chennai, Tamil Nadu, India. She was awarded the best outgoing student award in her department (ECE) in 2015. She did an internship at TATA Power SED, Bangalore, India during the summer of 2015. She then pursued Master of Science degree in Electrical Engineering as a graduate student at Missouri University of Science and Technology at Rolla, MO, USA. She performed her thesis under the guidance of Dr. Jie Huang. She did a co-op with Esdemc Technology LLC, Rolla, MO and an internship with Molex at Lisle, IL during the spring and summer of 2017 respectively. In May 2018, she received her Master's degree in Electrical Engineering from Missouri S&T.